Elevating Wind Energy Harvesting with J-shaped Blades: A CFD-driven Analysis of H-Darrieus Vertical Axis Wind Turbines

Ahmed Abdallah [1], Micheal A. William [2] and Iham F. Zidane [3]

(1) Electrical Energy Engineering Department, College of Engineering and Technology, Arab Academy for Science, Technology and Maritime Transport, Smart Village Campus, Egypt

(2) Mechanical Engineering Department, College of Engineering and Technology, Arab Academy for Science, Technology and Maritime Transport, Smart Village Campus, Egypt

(3) Mechanical Engineering Department, College of Engineering and Technology, Arab Academy for Science. Technology and Maritime Transport, AASTMT, 1029 Abu Kir, Alexandria – Egypt

1. **ABSTRACT:** This research introduces a novel J-shaped aerofoil designed to enhance the performance of H-Darrieus Vertical Axis Wind Turbines (VAWTs). A comprehensive comparison is conducted between the J-shaped aerofoil and the standard NACA 0015 airfoil to assess their impact on turbine efficiency. The study employs a two-dimensional, incompressible, transient, and turbulent flow model to capture airflow around the turbine blades. Model verification and validation are carried out through systematic evaluation of various parameters, including mesh sizes, time steps, turbulent models, and discretization techniques.

Computational Fluid Dynamics (CFD) simulations give useful insights into the aerodynamic features of H-Darrieus VAWT blades, indicating greater performance of the J-shaped airfoil over conventional designs. Results suggest that blades with the J-shaped aerofoil demonstrate increased overall performance and, notably, a 142% increase in beginning torque compared to the normal NACA 0015 type. This research not only contributes a new and efficient aerofoil design for vertical axis wind turbines but also offers full knowledge of its aerodynamic benefits via rigorous simulation and analysis.

Nomenclature			
λ	tip speed ratio	∇	curl
C_p	Coefficient of power	G	Gromeka acceleration vector (m/s^2)
u	Wind speed (m/s)	t	Time Step (s)
L	chord length (m)	ξ	vorticity vector $(1/s)$
ω	angular velocity (rad/s)	D	Turbine diameter (m)
R	turbine's radius (m)		
C_m	Moment coefficient		

2. INTRODUCTION

Energy shortages and environmental deterioration drive renewable energy demand. Due to technical advances, wind energy has a low environmental effect and low operational costs [1]. Wind turbines have a either horizontal or vertical axis. Large onshore and offshore projects require HAWTs, whereas suburban areas prefer VAWTs. Variable pitch control and blade airfoils are now suitable for large onshore and offshore applications [2].

VAWTs are great for unstable misalignment fluxes because of their omnidirectional design, low noise, and efficiency [3]. Savonius, Darrieus, and H-rotor Vertical Axis Wind Turbines (VAWTs) can be used in windy and urban locations. Despite being inefficient at low torques, the Savonius rotor self-starts.

Despite its better efficiency, the Darrieus rotor has poorer self-starting [2, 26]. The inherent appeal of H-rotors lies in their configuration featuring straight blades, facilitating wind capture from varied directions. Despite exhibiting a superior power coefficient relative to conventional Savonius rotors, the H-rotor's advancement has been impeded by its constrained self-starting capabilities. Studies have been carried out to increase the H-type wind turbines' ability to start independently [4].

A J-shaped blade was made by cutting a notch on one side of the blade and opening the trailing edge [5, 6] . Similar to conventional airfoils, this design delivers better overall efficiency after self-starting due to Darrieus-type blades and higher beginning torque because of the 'cup' form of Savonius-type blades. The design defines where the notch will go [5, 6].

Studies on J-shaped airfoils have shown that by creating a cut in the outer part of the blade, a notch on the airfoil may increase the torque needed for starting and improve VAWTs' ability to start themselves. [5]. But under usual operating settings, this can also result in a loss in turbine performance. Zamani et al. [6, 7] examined a turbine with NACA0015-based blades and DU 06-W-200 airfoils in 2D and 3D and compared the outcomes with similar J-shaped-based turbines. Observing the spinning of 3D NACA-based blades, it was discovered that they exhibited negative torque values, a behavior that might potentially be ascribed to stall effects. The J-shaped airfoils generated an average greater torque with no negative values, but the fatigue stress and vibrations on the blades were reduced to the ideal λ value of $\lambda = 1.6$.

According to a study on Darrieus-type (VAWTs), utilizing a blade design with a J shape does not increase performance and is not suggested [8]. Contrary to the original circumstances employed in the articles, the study focused on turbines operating in the high λ zone with solidity values between 0.1 and 0.2. The influence of λ and solidity on the functioning of Darrieus VAWTs was investigated further. There are two primary operational zones taken into consideration: low λ ($\lambda = 1.5$) and high λ ($\lambda = 5$ or 6) [9]. Narrower operating zones and dynamic stall effects originate from a greater angle of attack on the airfoil when λ is in the low area. Thus, low λ and high solidity (usually between 0.3 and 0.5) appear to be favorable for the J-shaped form.

This research aims to create an optimized J-shaped blade to enhance the Darrieus turbine's performance by encouraging resilient, sustainable infrastructure that is built and run to have the least negative effects on the environment that maintains the Darrieus turbine's performance while improving starting torque, utilizing a NACA0015 airfoil as a model. The earlier research on J-shapes [5-7] and the more recent study [10] concentrated on blades with a hollow and hair-like form; however, they did not investigate the inner shape of the construction. Thus, this study evaluates the performance of J-shaped blades with an interior-filled construction.

3. PROBLEM DESCRIPTION AND SETUP

This study leverages the Finite Volume Fluent Solver to meticulously investigate the impact of J-shaped configurations on the aerodynamic performance of airfoils for vertical axis wind turbines, employing the Unsteady Reynolds Averaged Navier Stokes (URANS) governing equations. The research endeavors to contribute to the understanding of these configurations by presenting a comprehensive analysis through a turbulent, incompressible, and two-dimensional flow model.

This section initially summarizes the technique used to calculate the coefficient of momentum (Cm) and the Gromeka acceleration vector. It then compares the findings of the numerical model with those acquired from wind tunnel testing. It was next, adopting a J-shape configuration.

3.1 H-Darrieus wind turbine geometry features

The setup was equivalent to that of [6,7,11,12,13,14,27,28]. The J-shaped airfoil's cavity size and placement were determined based on very similar studies carried out in [6,24, 15]. Table 1 displays the parameters of the model. The middle shaft has been skipped in the current work, as it was left out of every study that had been released earlier on the same VAWT.

Currently, there is a wide range of Computational Fluid Dynamics (CFD) solvers, software for producing meshes, and tools for visualizing data. There are two types of software available: commercial and free/open source. Currently, ANSYS is the most widely used software for computational fluid dynamics (CFD), with over 40% of the market share. ANSYS includes two primary codes: CFX, which was purchased in 2003, and FLUENT, which was bought in 2006. Among open-source CFD tools, OpenFOAM from the ESI Group is the most popular.

This simulation was carried out using ANSYS FLUENT, as it has been in earlier research [6, 7, 11, 14,27,28]. According to [11], Ansys was compared to various CFD solvers with different validation models. Ansys is a perfect fit for experimental models.

Table 1. Main geometrical rotor characteristics

Characteristics	Details
No. of blades	3
Rated power	3.5 kW
Chord length	0.4 m
Turbine radius	1.25 m
Blade profile	NACA0015
Solidity	0.48
Wind speed	10 m/s
Reynolds no.	416,254

3.2 Wind turbine governing parameters

The three blades' combined moment coefficients are utilized to estimate the overall moment coefficient in the numerical model. To anticipate the global efficiency of the turbine, the values of the fluctuating moment coefficient are averaged. Since it is a transitory condition, the solution is not yet stable; hence, the transient effect cannot be considered during the first three cycles. The validity of the model in this study has been examined by a comparison of the coefficient of power (C_p) vs. tip speed ratio (λ) curve with findings reported in previous studies. The following formula is used to get the C_p from the moment

coefficient (C_m) value that was previously computed:

$$C_p = C_m (\omega L)/u \qquad (1)$$

where , L, and ω stand for the wind speed, reference length, and rotor angular velocity, respectively. According to [14], the value of L equals the turbine's radius (R) in a two-dimensional turbine simulation. By replacement, Equation (1) becomes

$$C_p = C_m (\omega R)/u \qquad (2)$$

However, the formula for the tip speed ratio (λ) is:

$$\lambda = (\omega R)/u \qquad (3)$$

The last equation that was utilized to derive the (C_p) from the averaged (C_m) determined value as follows, which serves to validate the numerical results:

$$C_p = C_m \lambda \qquad (4)$$

The Gromeka acceleration vector patterns around and within the wake of the airfoil were examined to understand how the J-blade affects aerodynamic performance. Accordingly, various aerodynamic phenomena have been examined and studied. Gromeka acceleration vector (m/s^2) is the rate of change of angular momentum [16]. According to [17], The total external torque acting on a system of particles equals the rate of change of the system's total angular momentum. The torque created on the turbine is evaluated by measuring the Gromeka acceleration vector.

For a 2D flow, the velocity (u) may be defined as

$$\vec{u} = \begin{pmatrix} u \\ v \\ 0 \end{pmatrix} \qquad (5)$$

And we can determine vorticity using equation (6).

$$\vec{\xi} = \nabla \times \vec{u} = \begin{pmatrix} \xi_x \\ \xi_y \\ \xi_z \end{pmatrix} \qquad (6)$$

For a 2D flow, the vorticity vector is always normal to the flow field plane. So the sole remaining component is the z component, defined as

$$\vec{\xi} = \nabla \times \vec{u} = \begin{pmatrix} 0 \\ 0 \\ \frac{\partial v}{\partial x} - \frac{\partial u}{\partial y} \end{pmatrix} \qquad (7)$$

To extract the Gromeka acceleration vector from the vorticity and velocity numbers that were previously calculated, the following equation is used:

$$\vec{G} = \vec{\xi} \times \vec{u} \qquad (8)$$

For a 2D flow, the Gromeka acceleration vector may be defined as

$$\vec{G} = \begin{pmatrix} v\xi_z \\ -u\xi_z \\ 0 \end{pmatrix} = \begin{pmatrix} v(\frac{\partial v}{\partial x} - \frac{\partial u}{\partial y}) \\ -uv(\frac{\partial v}{\partial x} - \frac{\partial u}{\partial y}) \\ 0 \end{pmatrix} \qquad (9)$$

To determine the Gromeka acceleration vector magnitude, this equation is utilized.

$$\overrightarrow{|G|} = \sqrt{\left(v\left(\frac{\partial v}{\partial x} - \frac{\partial u}{\partial y}\right)\right)^2 + \left(-u\left(\frac{\partial v}{\partial x} - \frac{\partial u}{\partial y}\right)\right)^2} \qquad (10)$$

$$= \sqrt{\left(\left(\frac{\partial v}{\partial x} - \frac{\partial u}{\partial y}\right)\right)^2 \times (u^2 + v^2)} \qquad (11)$$

$$= \sqrt{\left(|\vec{\xi}|\right)^2 \times (|\vec{u}|)^2} \qquad (12)$$

3.3 Numerical details and solver setup

The computational domain is shown in Figure 1 [11, 18]. The velocity inlet and pressure outlet boundary conditions were taken into account for the inlet and outlet of the computational domain, and the top and bottom limits were determined as symmetry. According to guidelines from the literature [19, 20], 10 m/s of air was pumped into the system throughout each simulation, and the turbulence intensity and turbulent viscosity ratio were kept at 0.1% and 10%, respectively, for all subsequent configurations. In wind tunnels, such low intensities are not unusual. For instance, at 10 m/s, the TU Delft wind tunnel has an I= 0.015% [21].

Through "interfaces," the two domains, rotating and stationary are connected using a sliding mesh approach. For the two side walls, two symmetric boundary conditions were used. Since they produced good results throughout the model validation process, they were left unchanged in all runs.

In each case, the mesh quality was checked. The range of values for the dimensionless wall distance Y plus (Y +) via the turbine blade airfoils was less than 1. Six μm was the initial grid height surrounding the airfoil.

Six meshes comprising 100,000 to 2 million cells were numerically evaluated. Daróczy et al., [11] The reference C_p value was compared with the retrieved C_p values at the turbine's claimed maximum efficiency, $\lambda = 1.6$. Figure 2 gives the C_p values of the 2D VAWT models, simulated using all mesh considerations for the NACA0015 airfoils. Mesh 5 is sufficient to converge the Cp to the desired level; an additional number of cells does not affect the result. Nevertheless, it is crucial to highlight a factual disparity existing between mesh 4 and mesh 5. Hence, Mesh 4 for CFD work was considered for the rest of the procedure to reduce the computation cost.
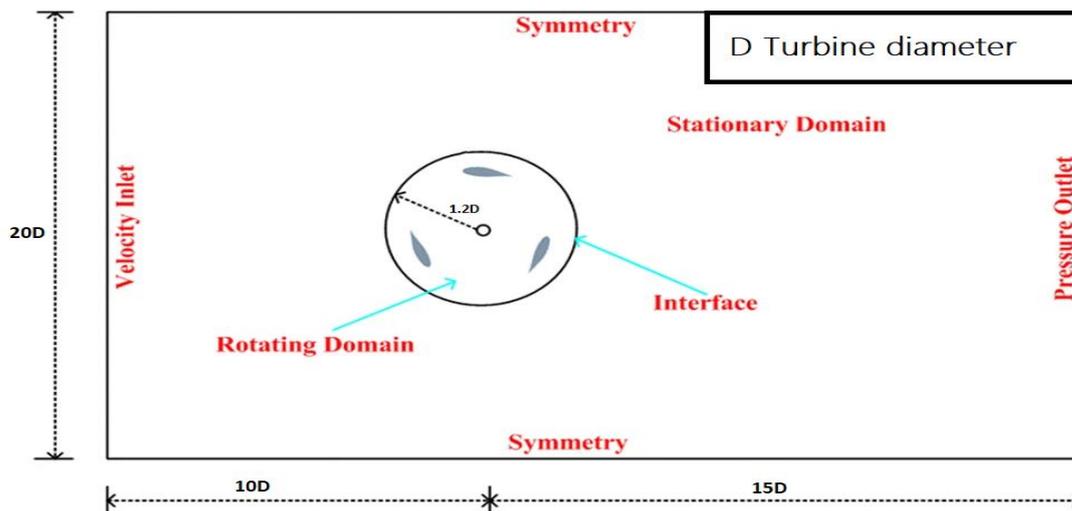

Figure 1. Computational domain

The results shown in Figure 2 are compared with the simulation data in Darócy et al., [11]. The results from Daróczy et al. [11] show about 1.2% of disparity with respect to the C_p levels attained by means of Mesh 4. This shows that Mesh 4 is easily deployable compared to mesh 5 and utilizes low processing power.
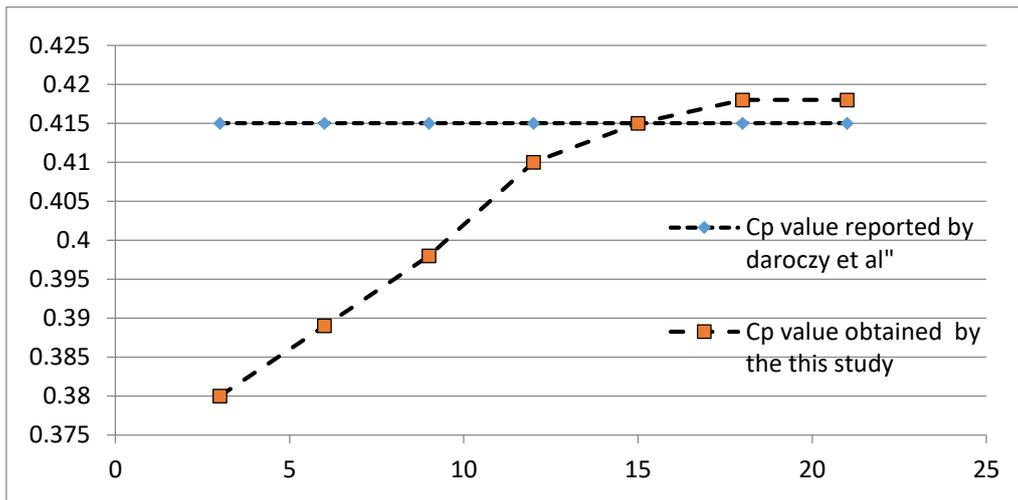
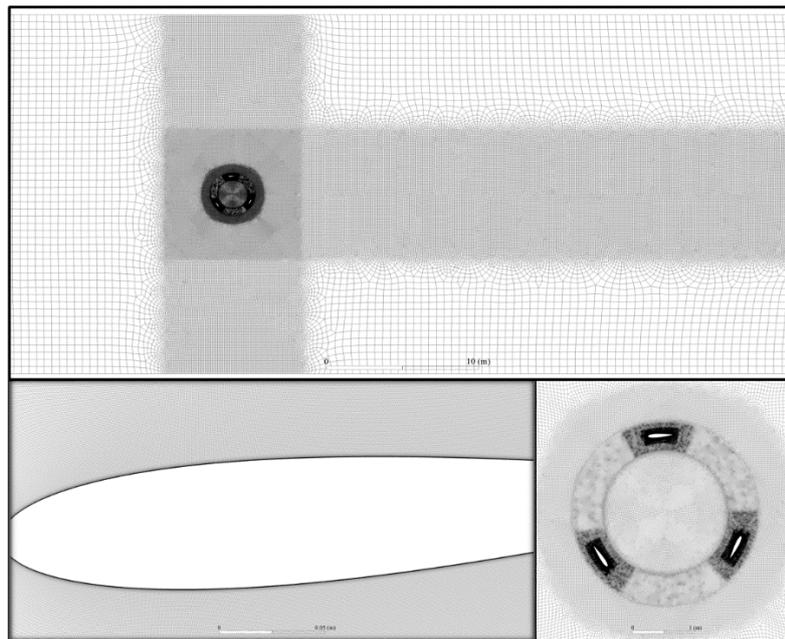**Figure 2.** Mesh independence study

Figure 3 . Grid distribution around NACA 0015

3.4 *Numerical setup*

The aerodynamic performance of the Darrieus VAWT was examined computationally at different angular velocities at an unchanged wind speed of 10 m/s. The numerical model applied in this work, according to Trivellato et al. [18], is based on a solution of the two-dimensional unsteady Reynolds

Averaged Navier-Stokes equations (U-RANS), and deals with the turbulent issue using the k-ω SST model. The coupled velocity–pressure scheme is solved via the SIMPLE algorithm [11]. Utilizing a second-order upwind approach, the dissipation ratio, momentum, and turbulent kinetic energy are computed. The outlet boundary is represented as a pressure outlet, the surface of the airfoil is described as a non slip wall., and the inlet boundary is represented as a velocity inlet.

Simulation assumptions, such as boundary conditions, are critical for CFD simulations because they specify the situation at the computational domain's boundaries. Non-slip walls, pressure outlets, velocity inlets, and interfaces are examples of these needs. The accuracy of the simulation results can be significantly influenced by the precise specification of these boundary conditions. For example, an incorrectly given input velocity might result in an inaccurate estimate of wind turbine performance. Furthermore, the chosen boundary conditions may have an impact on the simulation's stability and processing cost. This research makes use of boundary conditions from a variety of sources, including wall, outlet, inlet, and symmetry. The value of that for each boundary condition was assigned as [6,7,11,12,13,14].

Azimuthal increments served as the foundation for the transient simulation's time step. To replicate the five λ of interest, five unique rotating speeds w (rad/s) were considered: 0.2 (to examine the starting torque), 1.25, 1.6, 2 and 2.5.

The CFL (Courante-Fried-richse-Lewy) number can be used to compute the time step size. CFL = 1 is often recommended in CFD for stability [18,23]. However, substantially higher values are allowed with an implicit time integration technique. It has been established that meshes with variable-sized elements likewise exhibit a linear relationship between CFL number and numerical error; for both 1D and 2D difficulties, the numerical error points to a minimal value as the CFL number declines. Thus, the time step in the present investigation was defined as

$$\Delta t = 2\pi \, \Delta\theta / (360\omega) \qquad (13)$$

Where Δt time is step size and $\Delta\theta$ is azimuthal increment. (0.5 ^{0}) was utilized as the azimuthal increment at each time step in agreement with comparable numerical work published in [11]. Equation (13) was used to compute the appropriate time steps depending on the values of ω and $\Delta\theta$.

Table 2. ω and Δt for different λ.

λ	$\omega(rad/s)$	Time step (s)
0.2	1.6	0.005454
1.25	10	0.0008727
1.6	12.8	0.0006817
2	16	0.0005454
2.5	20	0.0004363

Figure 4 presents the results of a study conducted on the VAWT regarding the effects of the number of blade revolutions. It's evident that simulations with lower λ values need fewer rotations to obtain the C_p value's convergence than simulations with larger λ values. This supports findings from the literature, such as those found in [22,25]. Five rotations were applied at λ less than 1.25 and fifteen

rotations at λ more than 1.25 in order to reduce computation time and take into consideration Figure 4.
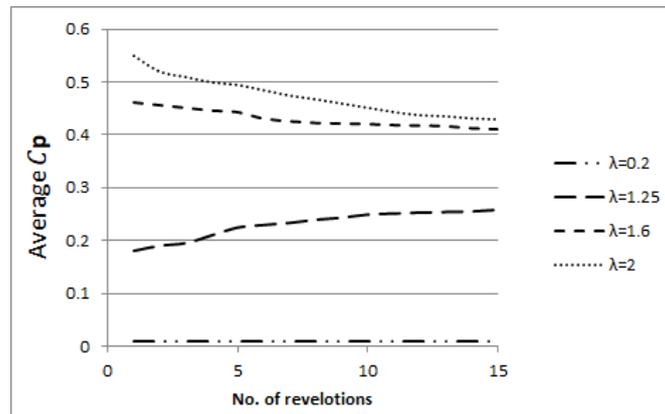

Figure 4. Number of revolutions until convergence of simulated Cp values at various λ.

4. VERIFICATION AND VALIDATION

Figure 5 presents a comparison between the C_p value results produced for the VAWT and Daróczy et al.'s numerical work. [11]
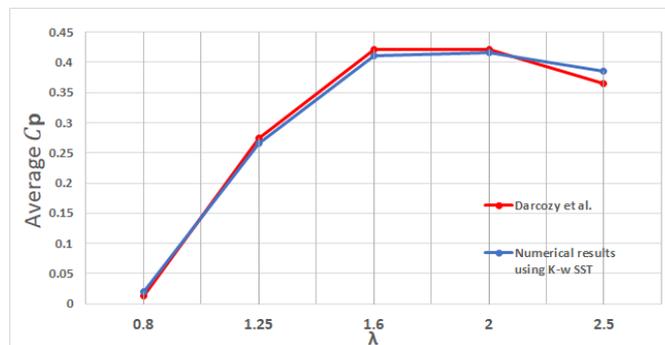

Figure 5. C_P comparison between the present study and Daróczy et al. at different λ

The simulated results from this study and those from Daróczy et al. [11] closely resemble each other. It is safe to rely on these results and proceed with applying the alteration, as there is an average error of 3.6%. When compared to experimental data from [23], authors in [6, 7] and [11] demonstrated that the k-ω SST model was accurate in producing good results. Therefore, the k-ω SST turbulence model was used.
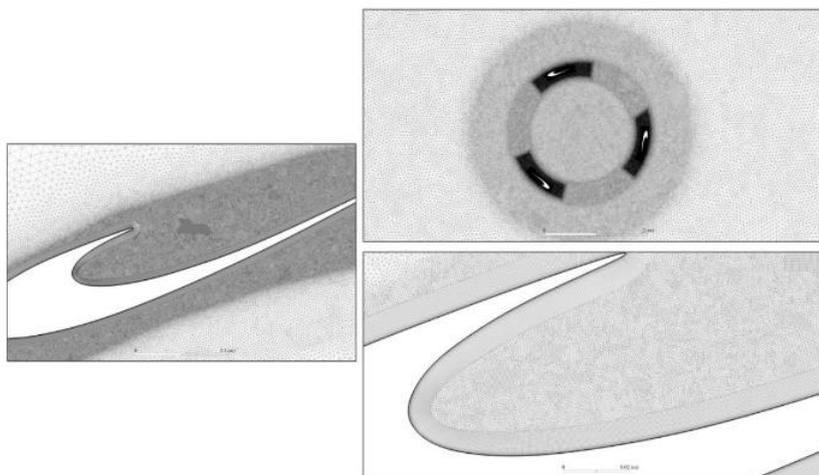
5. J-BLADE CONFGURATION

It is crucial to maintain the Darrieus turbine's performance in urban areas while increasing starting torque in order to improve the wind rotor's aerodynamic performance. A J-shaped design enhancement was suggested, as shown in figure 6, with an inner cut applied to a NACA0015 airfoil. To assess the

design under typical operating conditions, CFD simulations were run for the design for the λ values that were previously studied, namely λ = 1.25, 1.6, and 2.5, and for λ = 0.2 to investigate the starting torque. Examining and adjusting the mesh near the airfoil was necessary since taking away a section of the inner structure results in new places where the flow has to be processed. This was done to ensure that the k-ω SST turbulence model's requirements were still met and that a y+ value less than 1 was still obtained.

(a)

(b)

Figure 6.(a) J-blade airfoil design and (b) the grid distribution

6. RESULTS AND DISCUSSION

As stated previously, the starting torque was estimated with a very low λ = 0.2. The value of this quantity gives a transient simulation with very small time steps, which should be fairly comparable to that undisturbed.

The simulated airfoil reveals that the J-blade airfoil has a 142% increase in beginning torque compared to the NACA0015 airfoil, as shown in figure 7. This rise in initial torque originates from the airfoil's cut, which causes additional drag going through the leeward zone. Therefore, this influence on gromeka acceleration vector contours for the j-blade airfoil was examined.

In this innovative J-shaped blade design, a harmonious integration of lift and drag forces is achieved, strategically maximizing the capture of wind energy. A cut in the design allows air to capture and contribute to the lift generated by the laminar flow over the sleek surface of the blade. This intentional synergy between aerodynamic features enhances the overall efficiency of the blade for optimal wind energy utilization.

The J-blade consequently acts as a consequence of simultaneous lift and drag forces. In addition, the J-blade's notch provides drag force that helps the blades rotate more swiftly. Conversely, it enhances rotational efficiency by creating greater torque by harnessing the same wind more often.
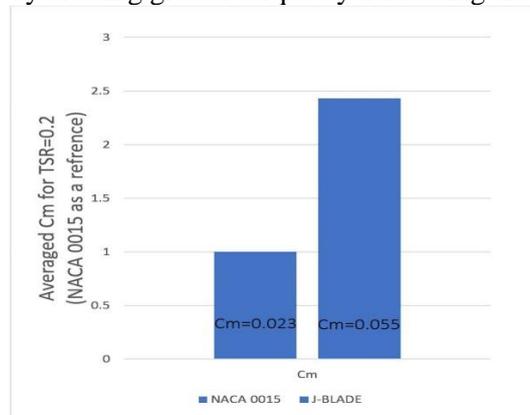

Figure 7. Averaged C_m for λ=0.2 of NACA0015 (left) and J-blade (Right)

For a very low λ, the leeward zone torque generated by the J-shape is enhanced, as seen in Figures 8, 9a, and 9b. The outlines depict how a vortex forms inside the airfoil, altering the direction of the outer flow and creating an increase in torque and angular momentum, which results in a drag boost. When the gromeka vector's x and y components are solved, it can be noticed that an increase in both the positive and negative components causes the resultant force to expand. The tangential component of this force aligns with the rotational direction, attributed to the "cup" shape, resembling the effect of a Savonius turbine. This configuration enhances the starting torque compared to the symmetrical NACA0015 air-foil. However, the overall drag of the J-blade increases due to heightened profile drag resulting from the transformation of the airfoil to the cup shape. This alteration induces boundary layer separation from the surface, aligning with insights and observations from existing literature [5, 6,13].
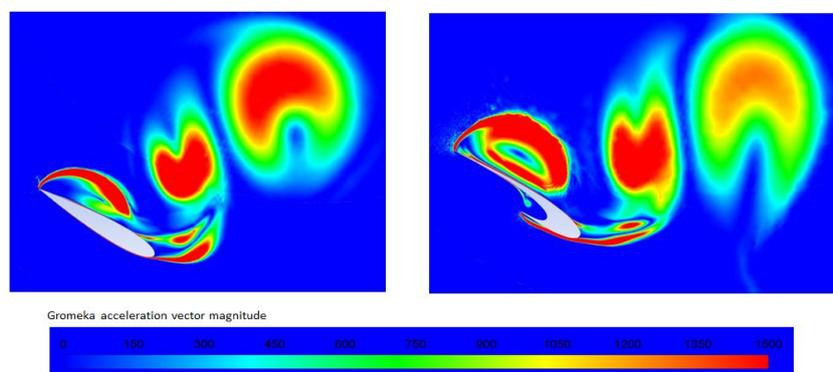

Figure 8. Contours of the Gromeka acceleration vector in leeward region at λ =0 .2 around the airfoil for NACA0015 (left) and J-blade (right)

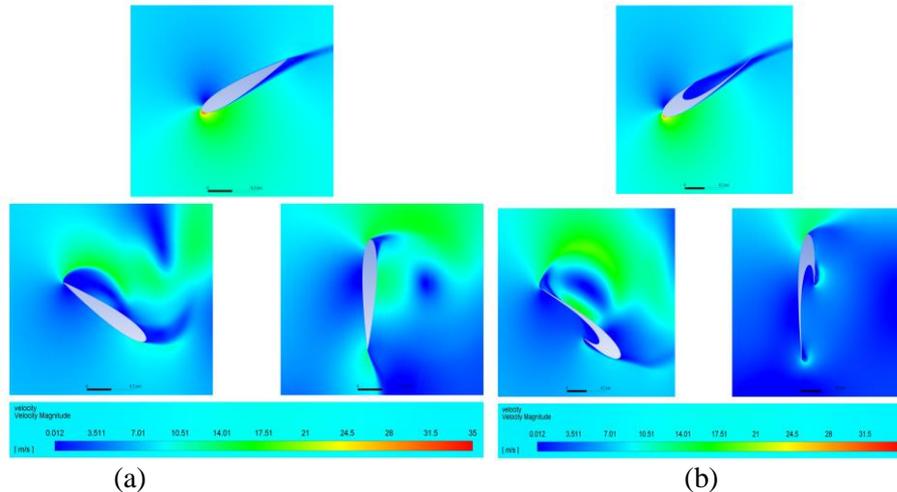<center>(a)</center> <center>(b)</center>

Figure 9 (a) contours of velocity magnitude λ =0.2 around turbine and blade for NACA0015 and (b) contours of velocity magnitude λ =0.2 around turbine and blade for J-blade

The torque values of the J-blade airfoil and the NACA0015 airfoil are comparable. For the majority of the operating zone, the J-blade airfoil outperformed the NACA0015 airfoil in terms of performance. The J-blade airfoil generated torque equivalent to the NACA0015 airfoil at λ of 1.25 and 1.6, but it was more uniform, which added benefits in terms of energy generation and mechanical stresses. Nevertheless, the J-blade airfoil's performance began to lag behind that of the NACA0015 airfoil at λ of 2.5.

The gromeka acceleration vector contours were examined in the leeward zone in order to have a deeper comprehension of the flow behavior surrounding the various airfoils. Examples of the findings for the airfoils in the leeward zone at the λ of their best performance (λ = 1.6) are shown in Figures 11a, 11b.

On the pressure side, the J-blade airfoil displays vortexes, yet the flow characteristics are not significantly affected by this cut. Figure 10b illustrates how the slight increase in drag causes just a slight reduction in torque in that area.

With regard to the contours in the leeward zone, both airfoils exhibit significant flow separation. It is noteworthy, however, that the J-blade design exhibits the lowest vortex production, as shown in Figures 11a, 11b.

A transitional separation bubble occurs when the boundary layer splits off the airfoil surface due to an unfavorable pressure gradient, as per the study presented by [13]. Figs. 11a, 11b.depict the flow separation phenomena that happened in the leeward zone with NACA0015 and J-blade. For each configuration, the highest power coefficient has been produced by using the ideal λ value for these Gromeka shapes. After the splitting of the laminar boundary layer, an extremely unstable unattached shear film arises, and turbulent flow transitions inside it. Due to the enhanced momentum conveyance of the turbulent flow, which promotes reattachment, a turbulent boundary layer forms downstream.

The boundary layer expands when a separation bubble forms, increasing the pressure drag of the airfoil. When there isn't a separation bubble, the airfoil's drag can increase by a factor of many above its baseline drag. A transitional separation bubble also affects lift, which may cause questions regarding the airfoil's overall aerodynamic performance. A J-blade with a shorter flow separation bubble contributes more flow particles to lift production, as the accompanying figures illustrate. Consequently, the VAWT aerodynamic performance is improved.

This is consistent with the earlier results shown in Figures 10a, 10b, and 10c, where NACA 0015 was

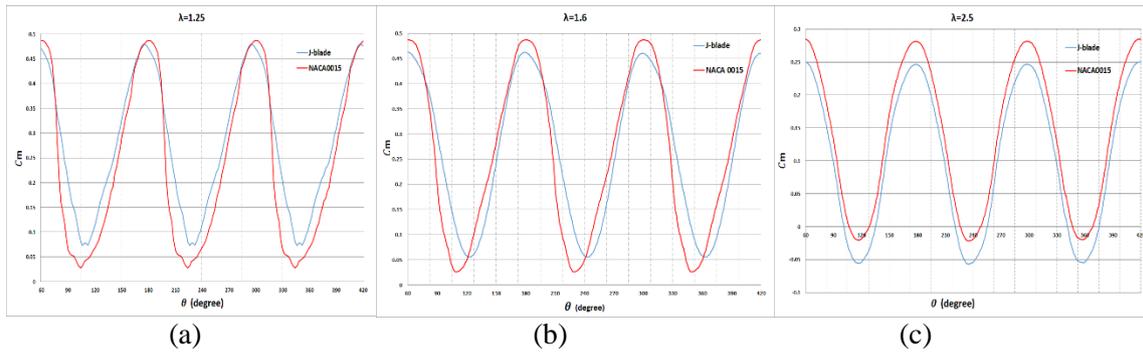greater than the lowest torque value for the J-blade produced in the leeward zone.

(a) (b) (c)

Figure 10. Cm comparison between NACA0015 (red) and J-blade (blue) at
λ =1.25(a), 1.6 (b), 2.5(c)

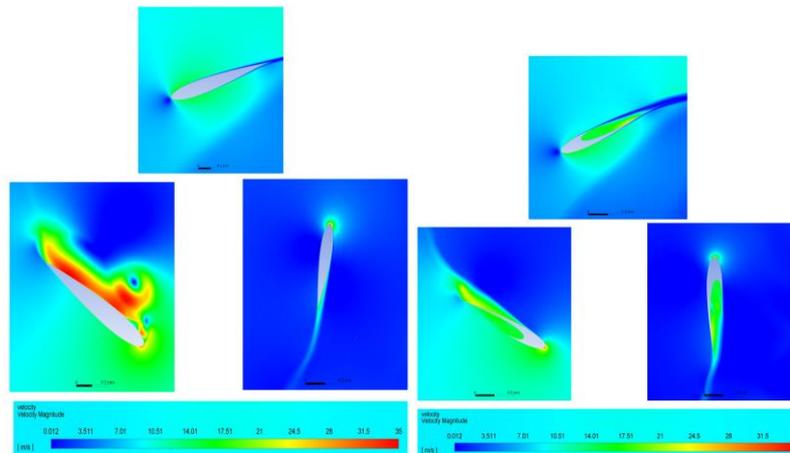
Figure 11 .(a) Contours of velocity magnitude λ =1.6 around turbine and blade for NACA0015 and
(b) Contours of velocity magnitude λ =1.6 around turbine and blade for J-blade
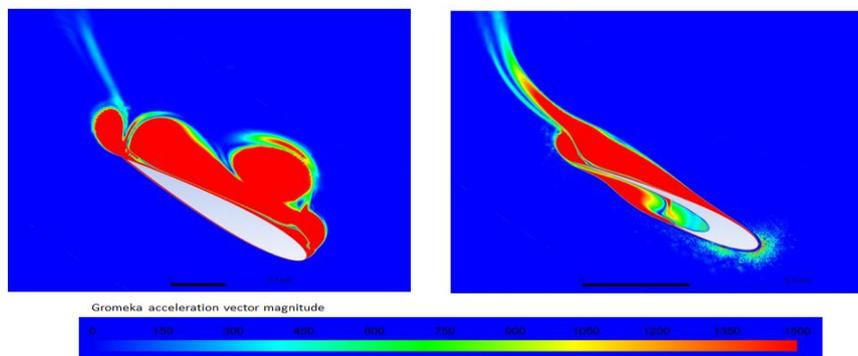

Figure 12. Contours of Gromeka acceleration vector magnitude in leeward region At λ =1.6
Around blade for NACA0015(left) and J-blade (right)

Thus, with λ = 1.6, Figure 13 displays examples of the turbulence fields for this airfoil. The vortex

shedding in the leeward zone is a substantial influence detected in the velocity field. The Gromeka acceleration vector contour charts given in Figure 12 indicate how the J-blade airfoil greatly lowers the creation of vortices and shedding during passage in the leeward zone. In Figure 13, the contour plots of turbulence intensity are provided to offer a more complete study of the effect of this vortex production. Consistent with past conversations, the NACA0015 airfoil is more sensitive to turbulence intensity in the leeward zone due of vortex formation and shedding.

As evidenced by the contours of turbulence intensity in Figure 13. There is less turbulence in the leeward region of the airfoil and more in the downwind area when comparing the J-blade airfoil case to the NACA0015 airfoil. Thus, combining both factors results in a uniform wake behind the turbine for the J-blade airfoil. Because turbulence from one turbine impacts the energy production of the next, we may use this consistency by deploying more and more wind turbines in the same geographical location, resulting in higher energy yields and cost savings. The instability in the wake raises the mechanical stresses and lowers the turbine's energy production.
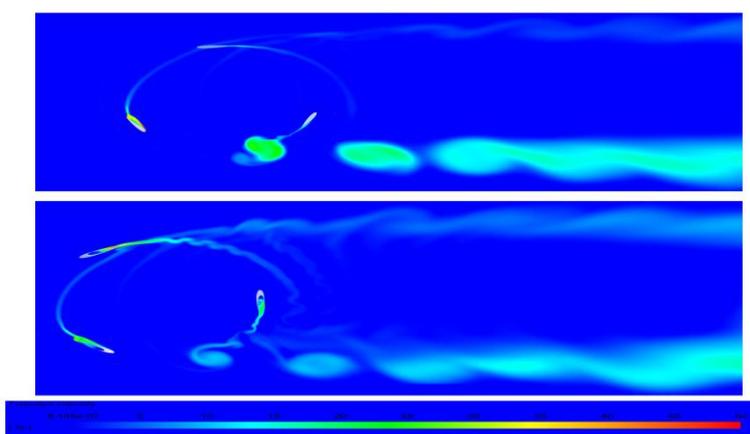

Figure 13. Contours of turbulence intensity λ =1.6 around the turbine for NACA0015 (upper) and J-blade (down)

7. CONCLUSIONS

This research introduces and investigates the performance of an enhanced J-shaped blade for the Darrieus turbine, specifically tailored to urban environments. Using the URANS governing equations, a turbulent, incompressible, two-dimensional flow model was developed, focusing on both experimental validation and numerical models. The study systematically compared the proposed J-shaped blade with traditional NACA0015 blades, reproducing the Darrieus turbine to validate the numerical model in the range of low λ (λ = 1.5). The findings reveal that:

(1) The J-shaped blade not only preserves power generation at the maximum efficiency point but also enhances uniformity, offering advantages in terms of fatigue stresses. This characteristic enables a more efficient placement of turbines in wind farms within the same land area.

(2) Crucially, the J-shaped blade demonstrated a remarkable improvement in starting torque, achieving a torque that is 142% larger than that of the NACA0015 airfoil. This enhancement positions the turbine as a more viable and efficient solution for urban settings, addressing the challenges associated with initial rotation in low-wind conditions.

In summary, the integration of the proposed J-shaped blade not only maintains the overall performance of the Darrius turbine but also brings substantial advancements in starting torque, making it a promising innovation for urban wind energy applications. The research offers significant perspectives for the development and enhancement of Vertical-axis wind turbines. Paving the way for more sustainable and effective energy solutions in diverse environmental contexts.

8. REFERENCES

(1) Zidane, Iham F, Khalid M Saqr, Greg Swadener, Xianghong Ma, and Mohamed F Shehadeh. "On the Role of Surface Roughness in the Aerodynamic Performance and Energy Conversion of Horizontal WindTurbine Blades: A Review." *International journal of energy research* 40, no. 15 (2016): 2054-77. **https://doi.org/10.1002/er.3580**

(2) Hau, Erich. *Wind Turbines: Fundamentals, Technologies, Application, Economics.* Springer Science & Business Media, 2013. https://**doi**.org/**10.1007/978-3-642-27151-9**

(3) Fischer, Gunter Reinald, Timoleon Kipouros, and Anthony Mark Savill. "Multi-Objective Optimisation of Horizontal Axis Wind Turbine Structure and Energy Production Using Aerofoil and Blade Properties as Design Variables." *Renewable Energy* 62 (2014): 506-15. https://doi.org/10.1016/j.renene.2013.08.009

(4) Bukala, Jakub, Krzysztof Damaziak, Krzysztof Kroszczynski, Marcin Krzeszowiec, and Jerzy Malachowski. "Investigation of Parameters Influencing the Efficiency of Small Wind Turbines." *Journal of Wind Engineering and Industrial Aerodynamics* 146 (2015): 29-38. https://doi.org/10.1016/j.jweia.2015.06.017

(5) Chen, Jian, Hongxing Yang, Mo Yang, and Hongtao Xu. "The Effect of the Opening Ratio and Location on the Performance of a Novel Vertical Axis Darrieus Turbine." *Energy* 89 (2015): 819-34. https://doi.org/10.1016/j.energy.2015.05.136

(6) Zamani, Mahdi, Mohammad Javad Maghrebi, and Seyed Rasoul Varedi. "Starting Torque Improvement Using J-Shaped Straight-Bladed Darrieus Vertical Axis Wind Turbine by Means of Numerical Simulation." *Renewable Energy* 95 (2016): 109-26. https://doi.org/10.1016/j.renene.2016.03.069

(7) Zamani, Mahdi, Saeed Nazari, Sajad A Moshizi, and Mohammad Javad Maghrebi. "Three Dimensional Simulation of J-Shaped Darrieus Vertical Axis Wind Turbine." *Energy* 116 (2016): 1243-55. https://doi.org/10.1016/j.energy.2016.10.031

(8) Mohamed, MH. "Criticism Study of J-Shaped Darrieus Wind Turbine: Performance Evaluation and Noise Generation Assessment." *Energy* 177 (2019): 367-85. https://doi.org/10.1016/j.energy.2019.04.102

(9) Rezaeiha, Abdolrahim, Hamid Montazeri, and Bert Blocken. "Towards Optimal Aerodynamic Design of Vertical Axis Wind Turbines: Impact of Solidity and Number of Blades." *Energy* 165 (2018): 1129-48. https://doi.org/10.1016/j.energy.2018.09.192

(10) Pan, Lin, Ze Zhu, Haodong Xiao, and Leichong Wang. "Numerical Analysis and Parameter Optimization of J-Shaped Blade on Offshore Vertical Axis Wind Turbine." *Energies* 14, no. 19 (2021): 6426. **https://doi.org/10.3390/en14196426**

(11) Daróczy, László, Gábor Janiga, Klaus Petrasch, Michael Webner, and Dominique Thévenin. "Comparative Analysis of Turbulence Models for the Aerodynamic Simulation of H-Darrieus Rotors." *Energy* 90 (2015): 680-90. https://doi.org/10.1016/j.energy.2015.07.102

(12) Zidane, Iham F, Khalid M Saqr, Greg Swadener, Xianghong Ma, and Mohamed F Shehadeh. "Computational Fluid Dynamics Study of Dusty Air Flow over Naca 63415 Airfoil for Wind Turbine Applications." *Jurnal Teknologi* 79, no. 7-3 (2017): 1-6. https://doi.org/10.11113/jt.v79.11877

(13) Zidane, IF, G Swadener, Khalid M Saqr, X Ma, and Mohamed F Shehadeh. "CFD Investigation of Transitional Separation Bubble Characteristics on Naca 63415 Airfoil at Low Reynolds Numbers." Paper presented at the Proceedings of the 25th UKACM Conference on Computational Mechanics, 2017.

(14) McLaren, K, S Tullis, and S Ziada. "Computational Fluid Dynamics Simulation of the Aerodynamics of a High Solidity, Small-Scale Vertical Axis Wind Turbine." *Wind Energy* 15, no. 3 (2012): 349-61. **https://doi.org/10.1002/we.472**

(15) Zhang, TT, Wei Huang, ZG Wang, and Li Yan. "A Study of Airfoil Parameterization, Modeling, and Optimization Based on the Computational Fluid Dynamics Method." *Journal of Zhejiang University-SCIENCE A (Applied Physics & Engineering)* 17, no. 8 (2016): 632-45. DOI:10.1631/jzus.A1500308

(16) Chen, Tao, and Tianshu Liu. "Lamb Dilatation and Its Hydrodynamic Viscous Flux in near-Wall Incompressible Flows." *Physica D: Nonlinear Phenomena* 448 (2023): 133730. https://doi.org/10.1016/j.physd.2023.133730

(17) Tatum, Jeremy. *Classical Mechanics*. LibreTexts, 2023.

(18) Trivellato, Filippo, and M Raciti Castelli. "On the Courant–Friedrichs–Lewy Criterion of Rotating Grids in 2d Vertical-Axis Wind Turbine Analysis." *Renewable Energy* 62 (2014): 53-62. https://doi.org/10.1016/j.renene.2013.06.022

(19) Lanzafame, Rosario, Stefano Mauro, and Michele Messina. "2d Cfd Modeling of H-Darrieus Wind Turbines Using a Transition Turbulence Model." *Energy Procedia* 45 (2014): 131-40. https://doi.org/10.1016/j.egypro.2014.01.015

(20) Langtry, Robin Blair. "A Correlation-Based Transition Model Using Local Variables for Unstructured Parallelized Cfd Codes." (2006). http://dx.doi.org/10.18419/opus-1705

(21) Ferreira, CJ Simao, GJW van Bussel, and GAM van Kuik. "2d Cfd Simulation of Dynamic Stall on a Vertical Axis Wind Turbine: Verification and Validation with Piv Measurements." Paper presented at the 45th AIAA Aerospace Sciences Meeting 2007, 8-11 January 2007, Reno, NV, 2007. 10.2514/6.2007-1367

(22) Maître, Thierry, Ervin Amet, and Christian Pellone. "Modeling of the Flow in a Darrieus Water Turbine: Wall Grid Refinement Analysis and Comparison with Experiments." *Renewable Energy* 51 (2013): 497-512. https://doi.org/10.1016/j.renene.2012.09.030

(23) Bravo, R, S Tullis, and S Ziada. "Performance Testing of a Small Vertical-Axis Wind Turbine." Paper presented at the Proceedings of the 21st Canadian Congress of Applied Mechanics, 2007.

(24) Zidane, Iham F, Greg Swadener, Xianghong Ma, Mohamed F Shehadeh, Mahmoud H Salem, and Khalid M Saqr. "Performance of a Wind Turbine Blade in Sandstorms Using a Cfd-Bem Based Neural Network." *Journal of Renewable and Sustainable Energy* 12, no. 5 (2020) https://doi.org/10.1063/5.0012272

(25) Zidane, Iham F, Hesham M Ali, Greg Swadener, Yehia A Eldrainy, and Ali I Shehata. "Effect of Upstream Deflector Utilization on H-Darrieus Wind Turbine Performance: An Optimization Study." *Alexandria Engineering Journal* 63 (2023): 175-89. https://doi.org/10.1016/j.aej.2022.07.052

(26) Radhakrishnan, Jayakrishnan, Surya Sridhar, Mohammed Zuber, Eddie YK Ng, and Satish Shenoy. "Design optimization of a Contra-Rotating VAWT: A comprehensive study using Taguchi method and CFD." Energy Conversion and Management 298 (2023): 117766. https://doi.org/10.1016/j.enconman.2023.117766

(27) Afif, A. A., Putri Wulandari, and Ary Syahriar. "CFD analysis of vertical axis wind turbine using ansys fluent." In Journal of Physics: Conference Series, vol. 1517, no. 1, p. 012062. IOP Publishing, 2020. 10.1088/1742-6596/1517/1/012062

(28) Duty, Drusilla, Muhamad Johan, Yuwaraja Samy, Mohd Ezrin Indarah, Syahmi Shaharudin, Djamal Didane, and Bukhari Manshoor. 2023. "Performance Analysis of VAWT With H-Darrieus Rotor Using 2D CFD Modelling". Journal of Design for Sustainable and Environment 5 (1), 5-10. https://www.jdse.fazpublishing.com/index.php/jdse/article/view/44.